Recent Advances in Fibre Optic Array Technologies

Scott Foster, Alexei Tikhomirov, John van Velzen and Joanne Harrison

Defence Science and Technology Organisation, PO Box 1500, Edinburgh, Australia

ABSTRACT

An acoustic array technology based on distributed feedback fibre laser sensors is described. Details of an advanced fibre laser hydrophone based on a flexural beam "bender" mechanism are presented, including laboratory data demonstrating sea-state-zero acoustic sensitivity, excellent vibration rejection and a flat acoustic response over a bandwidth exceeding 5kHz. Details of the system architecture including the interferometric interrogation system are also presented and some of the key practical constraints on system performance discussed.

INTRODUCTION

The fibre optic hydrophone was first proposed by James Cole (Cole et al.1975) and is significant as one of the earliest applications of optical fibre. The first proof of principle demonstrations were achieved independently by two groups in 1977 (Cole et al. 1977, Bucaro et al. 1977) and, following substantial research and development during the 1980s and 90s, the technology has now progressed to the extent that the first operational, military fibre optic sonar systems are now appearing. The US Navy Virginia class submarines comissioned a large aperture fibre optic planar hull array in 2004 (Kirkendall et al. 2006).

Early investment in optical fibre hydrophones was stimulated by the apparent benefits of fiber optic telemetry as well as claims of a range of significant advantages over conventional piezoelectric sensor technology -- including increased sensitivity, geometric versatility, multi-influence sensing capability and immunity from EM interference (Giallorenzi et al. 1982). As the technology has developed over time, practical advantages such as multiplexing capability, reduction in weight and storage volume, ease of handling and increased reliability have emerged as the main drivers (Kirkendall and Dandridge 2004, Nash 1996).

With the rapid development of the photonics field in recent years (driven primarily by the telecommunications industry), a number of new technologies have emerged which offer orders of magnitude increase in intrinsic sensitivity (strain resolution per unit length of fibre exposed to the environment) over the conventional interferometric methods which have historically dominated fibre optic hydrophone development (Kirkendall and Dandridge 2004). Arguably, the most promising of these new techniqes is the fibre laser strain sensor (FLS) (Koo and Kersey 1995) which can resolve length fluctuations at close to the thermodynamic limit over interaction lengths of only a few mm (Foster et al. 2009, 2011, Cranch et al. 2008). This represents an improvement of at least two orders of magnitude over conventional techniques which typically require several metres of fibre to achieve comparable sensitivity. Another feature of FLS which distinguishes it from more conventional techniques is the ease with which wavelength division multiplexing of multiple sensors may be implemented (Koo and Kersey 1995), making it ideally suited to array applications such as sonar. In 2006 (Foster et al. 2006) dense wavelength division multiplexing of 16 lasers on a single optical fiber was demonstrated with no apparent impact on the sensor resolution.

In this paper, we shall outline the basic operating principles of a fibre laser sensor system and summarise recent advances at DSTO towards the development of a high performance FLS sonar system. We shall describe in detail some key features of an experimental 8-element seabed array system currently under development and expected to be completed in late 2012.

THE FIBRE LASER STRAIN SENSOR

An erbium doped distributed feedback fibre laser is a compact in-fibre device, typically around 5cm in length, formed by writing a periodic refractive index modulation (Bragg grating) into a short section of active (erbium doped) optical fibre (Fig. 1). Energy is supplied by *optically pumping* with an infra-red laser diode as shown in Figure 1. Note that only a small fraction of pump energy is absorbed by the laser, the remainder continuing along the optical fibre. The absorbed pump energy is converted by a non-linear optical amplification process into virtually single-wavelength infra-red laser output in a range between 1520nm and 1560nm (the so called C-band). The laser wavelength is determined by a resonance condition of the Bragg grating structure within the device and corresponds to the Bragg wavelength λ_b which is equal to twice the grating pitch. The wavelength of the laser can be selected at the time of fabrication by adjusting the pitch of the grating.

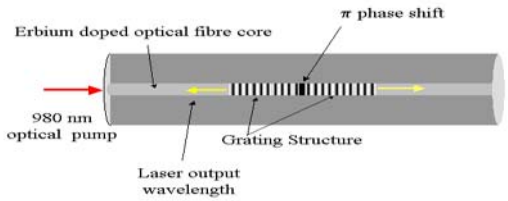

Figure 1. A Distributed feedback fibre laser.

The fibre laser sensor is based on the principle of measuring changes to laser wavelength caused by strain (Cranch et al. 2008). When the fibre is strained the pitch of the Bragg grating changes and the laser wavelength (or equivalently the

laser frequency) changes according to the approximate formula

$$\Delta\lambda/\lambda \cong \Delta\nu/\nu \cong \varepsilon \qquad (1)$$

Where λ and ν are the laser wavelength and frequency respectively, and ε is strain. The change in wavelength may be interrogated using optical interferometric methods (Kirkendall and Dandridge 2004) details of which shall be described later. Because the laser output is virtually monochromatic, very small wavelength shifts, and hence very small strains, may be detected. Indeed resolution of thermodynamic length fluctuations of the laser cavity in the order of 10^{-15}m/$\sqrt{}$Hz has been reported, corresponding to a strain resolution of 1 part in 10^{12} at frequencies ranging from a few Hz to above 10kHz (Foster et al. 2011). Thus, unlike more conventional interferometric sensor systems, sensitivity is essentially limited by the intrinsic thermodynamic noise of the sensor element, rather than the noise floor of the detection system. This is because of the remarkable stability of the distributed feedback (DFB) fibre laser (FL), and because, as will be seen when we discuss demodulation in more detail below, the sensitivity of the interrogating interferometer can always be increased to ensure that laser frequency noise exceeds the noise floor of the detection system.

A key feature of fibre laser sensing is the simplicity of multiplexing (Koo and Kersey 1995). The essential features of a wavelength division multiplexed (WDM) fibre laser sensor architecture can be seen in Figure 2 which shows a schematic of the (8-channel) acoustic array system currently being developed at DSTO. Laser sensors of different wavelengths are arranged serially along an optical fibre and pumped remotely by a single (1480nm) pump source. The multiple laser outputs, carrying the sensor information, return along the same fibre that delivers the pump. Since light waves of differing wavelengths do not interfere, a single interferometer is sufficient to enable demodulation of each of the signals from the multiple sensors. The light is split into its constituent wavelength components (corresponding to the sensor channels) by a dispersive optical component before the intensity on each channel is recorded by an array of photodetectors. Note that the only part of this system deployed to the environment is the array of laser sensors itself and the connecting optical fibre, which for our system may be up to 5km in length.

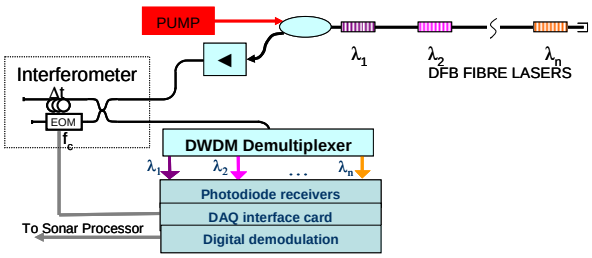

Figure 2. Multiplexed fibre laser array system.

Until recently, it was believed that high pump losses at the lasers severely limited the number of sensors that could be practically multiplexed in series. However, advances in DFB FL technology reported by the authors (Foster et al. 2006) showed for the first time that losses well below 0.5dB per device are achievable, suggesting that bandwidth limited sensor counts in the 50+ element range are practically realisable with quite modest power requirements. A 16 element DFB FL sensor array with no significant degradation in noise performance compared to a single channel system has previously been demonstrated (Foster et al. 2006).

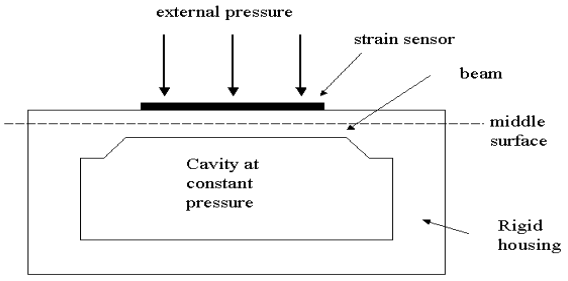

Figure 3. An acoustic bender. External pressure changes cause the beam to flex, straining the upper and lower surfaces.

THE ACOUSTIC TRANSDUCER

Early attempts to develop an FLS hydrophone were unsuccessful due to low pressure sensitivity and poor mechanical stability (Hill et al. 1999). We have developed an approach based on a flexural bender arrangement (Figure 2) where the laser is bonded to one edge of a flexible beam which deforms under the influence of external pressure changes (Foster et al. 2005, 2011). Compared to alternative approaches, this arrangement has a number of advantages including simplicity, exceptional mechanical stability and decoupling of pressure sensitivity from fibre material parameters.

The beam displacement is determined by the differential equation

$$\frac{\partial^2 y}{\partial t^2} + \frac{T^2 E}{12\rho}\frac{\partial^4 y}{dz^4} = F \qquad (2)$$

Where $y(z)$ is the transverse displacement of the beam middle surface at the point z along its axis, T is the beam thickness, E and ρ are material parameters of the beam, and F is an external forcing term which may be due to pressure or some other influence. From this equation it is possible to calculate all important hydrophone performance characteristics including pressure responsivity, acceleration rejection, and acoustic bandwidth – dependent only on the material and geometric parameters of the beam. This results in a highly versatile platform for sensor design.

The key performance parameter is pressure responsivity, given by (Foster et al. 2010):

$$\frac{\Delta\nu}{P} \cong \frac{3\nu L^2}{4T^2 E} \qquad (3)$$

Where P is the acoustic pressure and L is the beam length.

We fabricated our hydrophone from a pair of 0.5mm thick silicon wafers of width 8mm and length 70mm, bonded together to form a 1mm×8mm×70mm structure. A 15mm long by 1mm wide beam was fabricated in the upper wafer by means of a potassium hydroxide (KOH) wet etching process. A recess was etched in the lower wafer which enabled movement of the beam and formed the internal cavity. A groove was cut on the lower side of the upper plate (the beam) into which a DFB fibre laser was uniformly bonded. A thin poly-

mer sheet was bonded to the upper surface of the top plate providing a seal to the internal volume. The assembled structure is shown in Figure 4.

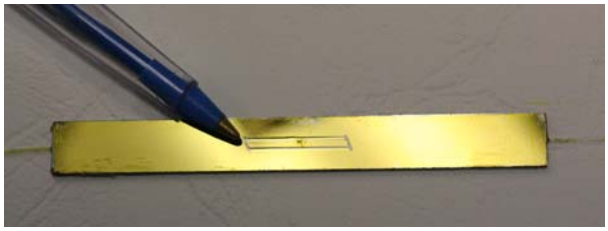

Figure 4. The assembled fibre laser hydrophone.

The hydrophone displays excellent acoustic performance, with a flat response of 107dB re Hz/Pa over a band exceeding 5kHz as shown in Figure 5. This responsivity results in a noise equivalent pressure (NEP) of about 40dB re µPa/√Hz at 1kHz which is below the lowest ambient ocean noise (Fig. 6). The exceptionally flat response is due to the high resonant frequency of the beam (about 15kHz in-air) which also results in very good vibration rejection.

Due to fluid loading, the beam resonance is reduced to 9kHz in-water as is clearly evident from the solid curve in Figure 5. The weak spectral feature at 4kHz is believed to be the first structural resonance of the outer hydrophone body. This indicates that the body (which should ideally be rigid) may require additional reinforcement to optimise high frequency performance. This can be achieved by mounting in a rigid secondry housing which would form part of an integrated array structure. Work on integration of the hydrophone into a seabed array system with an overall 5kHz bandwidth is currently underway. Field testing of an earlier FLS seabed array with a relatively lower (1kHz) bandwidth was reported previously (Goodman et al. 2009).

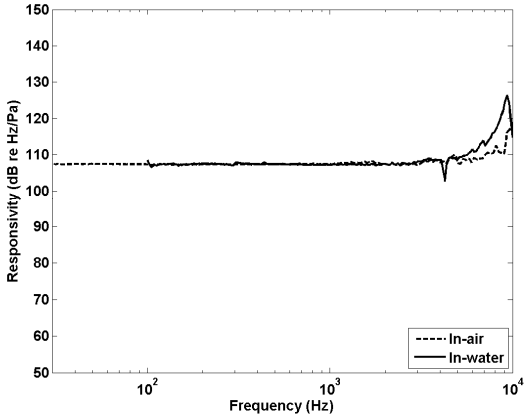

Figure 5. Measured responsivity of FLS hydrophone.

INTERFEROMETRIC DEMODULATION

Since the signal from a fibre laser sensor is encoded as a frequency (wavelength) modulation on an optical carrier the decoding (demodulation) of the signal component is a critical factor in determining the overall signal performance. The language of digital demodulation will be unfamiliar to many specialists in acoustics but is critical to understanding the performance limitations and design constraints of optical sonar systems in practice.

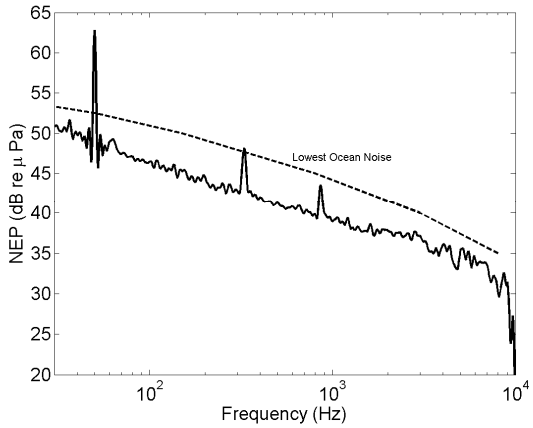

Figure 6. Acoustic noise floor of FLS hydrophone shown in comparison to ambient ocean noise (Cato 1997).

Figure 7 shows a simplified schematic of the Michelson interferometer arrangement used to demodulate our signal. This diagram may be considered to be a detail of the box marked "interferometer" in Figure 2 (coupled to a single photodetector). In simple terms, the purpose of the interferometer is to convert wavelength fluctuations on an optical signal into intensity fluctuations on an electrical current.

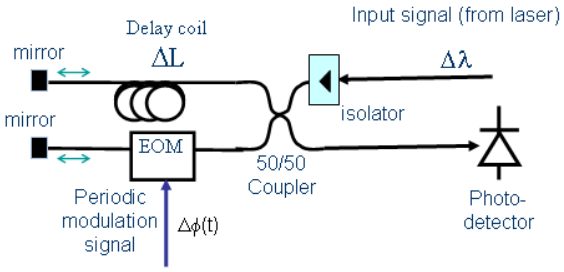

Figure 7. Simplified illustration of interferometric demodulation. EOM stands for electro-optic modulator.

Incident light from the laser (sensor) is split into two paths by an optical coupler. The light in each "arm" is reflected from end mirrors and recombined at the coupler and the resultant optical power measured by the photodetector. Unless the two beams are perfectly in-phase they destructively interfere and, as a consequence, the photodetector current is modulated by the path imbalance between the two arms of the interferometer. In particular, if a delay coil of length ΔL is placed in one arm of the interferometer (and all else being equal) the photodetector current takes the form:

$$I = I_0 + A\cos(4\pi\Delta L\,\nu / c) \qquad (4)$$

Where c is the speed of light in the optical fibre and ν is the laser frequency. If the laser frequency is of the form $\nu=\nu_0+\Delta\nu(t)$ where $\Delta\nu(t)$ is the signal of interest then

$$I = I_0 + A\cos(\phi_0 + 4\pi\Delta L\Delta\nu(t) / c) \qquad (5)$$

where ϕ_0 is a constant phase offset. Thus our signal of interest becomes encoded as a phase modulation on a (DC) electrical signal. The problem with (5) is that the change in current for a given change in frequency depends on ϕ_0 which is

unknown (and in fact drifts slowly over time). In pactice, it is much more convenient to encode the phase information on an RF carrier. This is done by injecting a *known* phase modulation $\Delta\phi(t)$ into the interferometer at some RF frequency f_c. Then we get

$$I = I_0 + A\cos(\phi_0 + \Delta\phi(t) + 4\pi\Delta L\Delta\nu(t)/c) \quad (6)$$

Note that we have not yet actually demodulated our signal, but have merely transferred it from an optical carrier to an RF (electrical) carrier. The carrier waveform is dependent on the specifics of the demodulation algorithm to be used. In the commonly used phase generated carrier (PGC) technique a sinusoidal modulation is injected into one arm of the interferometer (typically using a piezo-electric stretcher) and the quadrature phase components read off of the measured harmonics of the carrier in the Fourier domain (Kirkendall and Dandridge 2004). As with most RF phase modulation techniques, PGC requires calibration to a single optical wavelength and is therefore not suited to simultaneous demodulation of multiple signals carried on different wavelengths as required by our WDM architecture (Fig. 2). On the other hand, heterodyne techniques -- which use an acousto-optic modulator (AOM) to inject a constant frequency shift (equivalent to a "sawtooth" phase modulation) in one arm -- are wavelength insensitive but the high voltage signal generators needed to drive the AOM consume high power and tend to inject noise into the system.

To overcome these limitations we have developed a discrete 4-step digital phase stepping technique adapted from spatial interferometry (Schwider et al. 1993). Since in this method demodulation is performed subsequent to analogue-to-digital conversion, it is best to consider the algorithm from the point of view of discrete signal processing.

Consider a sequency of N samples taken over a short time interval T_c such that $T_c << 1/f_{max}$ where f_{max} is the information bandwidth of the signal (i.e. T_c is small enough that the measurand can be considered constant during the sampling interval). The n^{th} sample may be written as

$$I_n = I_0 + A\cos(\Delta\phi_n + \phi) \quad (7)$$

Where $\phi=\phi_0+4\pi\Delta L\Delta\nu/c$ is the unknown phase and ϕ_n is the *known* phase modulation at the time of the n^{th} sample. For a single sample, (7) may be viewed as an equation in 3 unknowns: I_0, A and ϕ. It thus follows that a minimum of 3 discrete samples are needed to obtain a single demodulated phase measurement. By utilising 4 samples per carrier cycle, our algorithm incorporates the *minimum degree of redundancy* necessary to achieve robustness against phase errors. In particular, suppose N=4 and

$$\phi_n = \frac{n\pi}{2}, \quad n=0\ldots3 \quad (8)$$

Then it can be shown (Schwider *et al.* 1993) that a robust estimation of phase is obtained from the formula

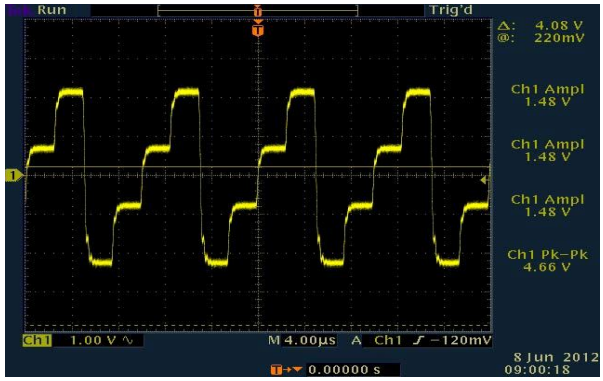

Figure 8. EOM drive voltage showing staircase waveform with period f_c=100kHz. To convert to phase use $\Delta\phi$=1.12ΔV.

$$\phi = \arctan\left(\frac{3I_1 - (I_0 + I_2 + I_3)}{(I_0 + I_1 + I_3) - 3I_2}\right) \quad (9)$$

The sequence of phase offsets (8) is repeated periodically at a frequency $f_c=1/T_c$ (or less) to obtain an oversampled time series for $\phi(t)$ which may then be low-pass filtered and down sampled to the desired acoustic bandwidth and exported to an audio device or sonar processor. Note that the unknown phase offset ϕ_0 merely manifests as a DC bias and is eliminated once high pass filering is performed. The remainder of ϕ is directly proportional to $\Delta\nu$ and hence (notwithstanding various noise contributions) to the acoustic pressure via (3).

To implement the above scheme we used an electro-optic phase modulator (EOM) in the interferometer (Fig. 8) which has the advantage of very low power requirements and high bandwidth (10GHz). This enables an unprecedented degree of flexibility in the choice of carrier waveform. Figure 8 shows the 4-step "staircase" waveform we generated to drive the EOM. Each voltage step corresponds to an equivalent phase step of approximately $\pi/2$ in the EOM. However, the EOM phase for a given voltage has a linear dependence on optical wavelength and varies by up to a few percent over the erbium C-band. The power of (9) is that it is insensitive to first order deviations of the phase from the nominal $\pi/2$ steps in (8), enabling simultaneous demodulation of multiple laser wavelengths, as required by Figure 2, without introducing distortion.

Since sampling only occurs at a single discrete time in each phase step, there is some flexibility in the design of the analogue waveform. The advantage of the staircase is that it is relatively insensitive to timing jitter and waveform distortion from slew rate limitations. However, it requires relatively high bandwidth drive electronics to implement.

Having outlined our basic method we shall now discuss how the choice of the carrier frequency f_c and path imbalance ΔL relate to system performance. Our objective was to achieve laser limited noise performance and high system dynamic range over a 5kHz acoustic bandwidth. As with all RF phase detection methods the system constraints may be summarised by Carson's Rule, which specifies the minimum carrier frequency required to achieve a specified detection bandwidth with a specified maximum signal amplitude:

$$f_c \geq 2 f_d \left(1 + 4A_{\max} / \pi\right) \qquad (10)$$

Where f_d is the detection bandwidth (5kHz in our case) and A_{max} is the maximum signal amplitude in radians. For A_{max} small, (10) merely expresses the Nyquist sampling theorem (i.e. you need to sample at twice the desired bandwidth). For A_{max} large compared to π the phase becomes ambiguous and Carson's rule tells you how fast you need to sample in order to "unambiguously" unwrap the phase. If we specify the detector noise N over the bandwidth then (10) can be expressed in terms of dynamic range D:

$$f_c \geq 2 f_d \left(1 + 4ND / \pi\right) \approx \frac{8 f_d ND}{\pi} \qquad (11)$$

To measure the noise floor of our detector we balance the interferometer (set ΔL=0) so that the signal becomes insensitive to laser frequency fluctuations $\Delta\nu$ and measure the residual signal. We measure noise floors in the 1-10μrad√Hz range typically dominated by laser intensity noise[1] which (conservatively) gives N~500μrad over a 5kHz bandwidth. The physical limitations of our data-acquisition hardware limit our maximum carrier frequency to f_c ~ 200kHz (corresponding to a sampling rate of 800kHz). Thus, according to (11) the maximum available dynamic range of our detector is about 92dB.

The key point to note is that phase detection systems are extremely expensive in terms of sampling rate overhead. For a 200kHz carrier frequency the overall sampling rate is 80 times the Nyquist rate!

Finally, we need to put the detector performance in the context of overall sensor performance. From Figure 6 we see that the laser frequency noise limited sensor noise floor is about 5dB below usual lowest ocean noise. To achieve overall ocean noise limited performance we therefore require the detector to be laser frequency noise limited. By (6) the minimum detectable frequency shift for phase resolution ϕ_{min} is

$$\Delta\nu_{\min} = \frac{c\phi_{\min}}{4\pi\Delta L} \qquad (12)$$

The larger the path imbalance ΔL the more sensitive the detector is. However the resolution is ultimately limited by the intrinsic laser frequency noise $\Delta\nu_{rms}$. The system will be laser noise limited if

$$\Delta L > \frac{c\phi_{\min}}{4\pi\Delta\nu_{rms}} \qquad (13)$$

[1]Unfortunately, a proper discussion of laser intensity noise is beyond the scope of this paper. To minimise its impact we use a somewhat more elaborate 'symmetric' variant of the demodulation technique described above, which enables discrimination of intensity and phase fluctuations.

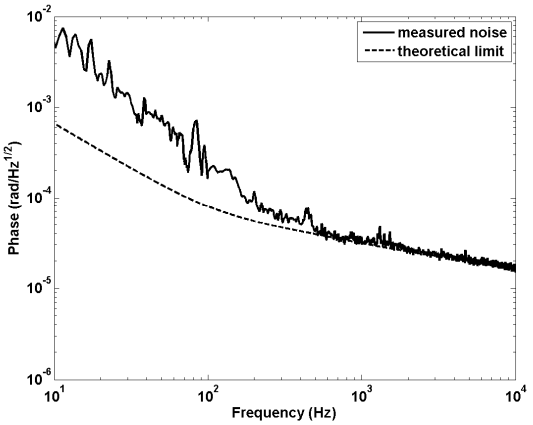

Figure 9. Measured phase noise of detection/demodulation system coupled to hydrophone in laboratory.

With a phase noise floor of up to 10μrad/√Hz and laser frequency noise (at 5kHz) of 10Hz/√Hz, we require a minimum path imbalance ΔL ~ 10m to achive laser noise limited (and hence ambient ocean noise limited) performance. Since the maximum detectable phase is fixed by Carsons Rule, any increase in the path imbalance beyond this figure comes at the cost of reducing dynamic range. In our system we have chosen a conservative value ΔL=20m.

Figure 9 shows a measured phase noise spectrum for (one channel of) our 8-channel detection/demodulation system coupled to a hydrophone in the laboratory. The dashed curve is the theoretical thermodynamic noise limit of the laser. Excess noise below 200Hz is believed to be residual acoustic background in the laboratory environment.

CONCLUSION

We have provided an overview of an emerging fibre optic acoustic array technology based on ultra-high resolution fibre laser strain sensors. Recent advances in the field have been described with reference to an experimental 8-element seabed array currently under construction at DSTO. We have given details of a high performance FLS hydrophone with acoustic resolution below usual lowest ocean noise and have described a novel digital demodulation scheme capable of robust, simultaneous demodulation of multiple WDM channels.

For reasons of brevity, we have glossed over many details of our system including the detection electronics, optical pump and WDM demultiplexing. These system components, although critical to performance, are in many respects standard and therefore less interesting in the current context. Also, we have not described integration of the hydrophone into an array module suitable for field deployment as this work is currently incomplete. We hope to report on these new developments, including the results of field trials, in the near future.

REFERENCES

Bucaro, J, Dardy, H and Carome, E 1977, 'Fiber-optic hydrophone', *J. Acoust. Soc. Am.*, vol. 62, pp. 1302-1304.

Cato, D 1997, 'Ambient sea noise in Australian waters', *Proceedings of the 5th International Congress on Sound and Vibration,* Adelaide, SA, p. 2813.

Cole, J, Johnson, R, Cuningham, J and Bhuta, P 1975, 'Optical detection of low frequency sound', *Proceedings of the Technical Program, Electro-optical Systems Design Conference, International Laser Exposition*, Anaheim, California, pp. 418-426.

Cole, J, Johnson, R and Bhuta, P 1977, 'Fiber-optic detection of sound', J. Acoust. Soc. Am., vol. 62, pp. 1136-1138.

Cranch, G, Flockhart, G and Kirkendall, C 2008, 'Distributed feedback fiber laser strain sensors', IEEE Sens. J., vol. 8, pp. 1161-1171.

Foster, S, Tikhomirov, A and Harrison, J 2011, 'Fundamental limits on low frequency cavity fluctuations in optical fibre lasers', *Conference on Lasers and Electro-Optics/Pacific Rim,* Sydney, Australia, Post-Deadline Session 2 (PD2).

Foster, S, Tikhomirov, A and van Velzen, J 2011, 'Towards a high performance fiber laser hydrophone', J. Lightwave, Tech., vol 29, pp. 1335-1342.

Foster, S, Cranch, G and Tikhomirov, A 2009, 'Experimental evidence for the thermal origin of 1/f frequency noise in erbium doped fiber lasers', Phys. Rev. A, vol. 79, p. 053802.

Foster, S, Tikhomirov, A, Englund, M, Inglis, H and Milnes, M 2006, 'A 16 channel fibre laser sensor array', *Proceedings of 18th International Conference on Optical Fiber Sensing (OFS18),* Cancun, Mexico, Paper FA4.

Foster, S, Tikhomirov, A, Milnes, M, van Velzen, J and Hardy, G 2005, 'A fibre laser hydrophone', Proc. SPIE, vol. 5855, pp. 627-630.

Giallorenzi, T, Bucaro, J, Dandridge, A, Sigel Jr, G, Cole, J, Rashleigh, S and Priest, R 1982, 'Optical Fiber Sensor Technology', IEEE J. Quant. Electron., vol. 18, pp. 626-665

Goodman, S, Foster, S, van Velzen, J and Mendis, H 2009, 'Field demonstration of a DFB fibre laser hydrophone seabed array off Jarvis Bay, Australia', Proc. SPIE, vol. 7503, p. 4L.

Hill, D, Nash, P, Jackson, D, Webb, D, 'Neill, S, Bennion, I and Zhang, I 1999, 'A Fibre Laser Hydrophone Array', Proc. SPIE, vol. 3860, pp. 55-66.

Kirkendall, C, Cole, J, Tveten, A. and Dandridge, A 2006, 'Progress in fiber optic acoustic and seismic sensing', *Proceedings of 18th International Conference on Optical Fiber Sensing (OFS18),* Cancun, Mexico.

Kirkendall, C and Dandridge, A 2004, 'Overview of high performance fibre-optic sensing', J. Phys. D:Applied Phys.**,** vol. 37**,** pp. R197-R216.

Koo, K and Kersey, A 1995, 'Fibre laser sensor with ultra-high strain resolution using interferometric interrogation', Electron. Lett., vol. 31, pp. 1180-1182.

Koo, K and Kersey, A 1995, Bragg grating based laser sensor systems with interferometric interrogation and wavelength division multiplexing', J. Lightwave Tech., vol. 13, pp. 1243-1249.

Nash, P 1996, 'Review of interferometric optical fibre hydrophone technology', IEE Proc.-Radar, Sonar, Navig., vol. 143**,** pp. 204-209.

Schwider, J, Falkenstorfer, O, Schreiber, H, Zoller, A and Streibl, N 1993 'New compensating four-phase algorithm for phase-shift interferometry', Optical Eng., vol. 32, pp. 1883-1885.